UC Davis
UC Davis Previously Published Works

Title

Gingiva-derived Stromal Cells Isolated from Cats Affected with Tooth Resorption Exhibit Increased Apoptosis, Inflammation, and Oxidative Stress while Experiencing Deteriorated Expansion and Anti-Oxidative Defense.

Permalink

https://escholarship.org/uc/item/5bv2d9cq

Journal

Stem cell reviews and reports, 19(5)

ISSN

2629-3269

Authors

Soltero-Rivera, Maria
Groborz, Sylwia
Janeczek, Maciej
et al.

Publication Date

2023-07-01

DOI

10.1007/s12015-023-10537-x

Peer reviewed

Gingiva-derived Stromal Cells Isolated from Cats Affected with Tooth Resorption Exhibit Increased Apoptosis, Inflammation, and Oxidative Stress while Experiencing Deteriorated Expansion and Anti-Oxidative Defense

Maria Soltero-Rivera[1] · Sylwia Groborz[2] · Maciej Janeczek[3] · Justyna Kornicka[2] · Monika Wierzgon[3] · Boaz Arzi[1,4] · Krzysztof Marycz[1,2,5]

Abstract

Gingiva-derived mesenchymal stromal cells (GMSCs) are multipotent cells characterized by multilineage differentiation potential, proliferative expansion, and unique immunomodulatory ability, making them attractive as a new treatment of periodontal regeneration. In this study, GMSCs obtained from the gingiva of healthy cats (HE) as well as from cats affected by tooth resorption (TR) were isolated and characterized. Feline GMSCs (fGMSCs) from HE patients exhibited fibroblast-like morphology, developed cellular body, specific growth pattern, high expansion, and proliferative potential as well as reduced senescence signature. fGMSCs demonstrated high s-100 and IL-10 positive cells, while simultaneously having low activity of IL-1. Moreover, high activity of ki-67 combined with reduced senescence markers were noted. In comparison, GMSCs from cats with TR exhibited enlarged nuclei and flat, irregular shape along with increased expression of CD44, s-100 and CD45 and downregulation of CD73. GMSCs from TR cats showed lower ability to form colonies, increased incidence of apoptosis, higher number of senescent cells, and reduced cell migration. Upregulation of pro-inflammatory cytokines was also noted in the TR group along with lower expression of mTOR and miR-17 and upregulation of miR-378. Mitochondrial dynamics, biogenesis and antioxidant properties are also negatively impacted in this group. Collectively, our findings suggest that GMSCs isolated from the gingiva of cats affected with TR have deteriorated functionality caused by impaired proliferation and growth and possibly mediated via mitochondrial dysfunction. fGMSCs or their EV's should be further investigated for their role in the pathophysiology of TR in cats.

Keywords Feline stem cells · Feline gingivostomatitis · Feline oral disorders

Abbreviations
GMSCs   Gingiva-Derived Mesenchymal Stromal Cells
fGMSCs Feline Gingiva-Derived Mesenchymal Stromal Cells
MSCs   Mesenchymal Stem Cells
TR   Tooth resorption
HE   Healthy

Krzysztof Marycz
kmmarycz@ucdavis.edu

1   Veterinary Surgical and Radiological Sciences, University of California, One Shields Avenue, Davis, CA 95616, USA

2   International Institute of Translational Medicine (MIMT), Jesionowa 16 Str, 55-114 Wisznia Mala, Poland

3   Department of Biostructure and Animal Physiology, Faculty of Veterinary Medicine, Wrocław University of Environmental and Life Sciences, Kozuchowska 1/3, 51-631 Wrocław, Poland

4   Veterinary Institute for Regenerative Cures, University of California, One Shields Avenue, Davis, CA 95616, USA

5   Department of Experimental Biology, Faculty of Biology and Animal Science, Wrocław University of Environmental and Life Sciences, Norwida 27B, 50-375 Wrocław, Poland

Introduction

Feline tooth resorptive lesions (TR), historically referred to as feline odontoclastic resorption lesions, are common lesions found in the teeth of 7 out of 10 domestic cats, increasing with age [1, 2]. Interestingly, the incidence of this disease in the wild feline population is much lower

[3–5]. Though the exact cause of TR has not been determined, a single infectious origin has been ruled out and *Lampropedia* species may have a contributing role [1, 6, 7]. Additionally, matrix metalloproteinase-9 (MMP9) mRNA expression is increased suggesting its involvement in the progress of TR [8]. Another important piece of the puzzle recently elucidated is that peripheral blood odontoclasts from patients with and without TR will respond differently to vitamin D (1,25-dihydroxyvitamin D) and IL-6 both of which are factors that attract and activate these cells [9, 10]. Resorptive lesions are typically painful, once they reach above the gumline, and at that point teeth are extracted to prevent infections and fractures [11]. Multiple Idiopathic Cervical Root Resorption (MICRR) is an analogous form of external root resorption in adult humans. It is recognized that TR as well as MICRR start at the cemento-enamel junction, diffusely affect the oral cavity and that these two entities likely share the mechanisms and progression of osteoclastic/odontoclastic root resorption [12, 13]. A possible association with feline herpes virus-1 (FeHV-1) infection has also been postulated but has not been definitively confirmed [12, 13]. Consequently, there is clinical and scientific value in further evaluating the cellular components playing a role in TR in cats.

Gingiva-derived mesenchymal stromal cells (GMSCs) are multipotent stromal stem cells that express stem cell-related genes such as Oct-4, SSEA-4, and STRO-1. GMSCs have fibroblast-like spindle shape morphology and are characterized by a high proliferative potential. These cells are positive for MSC-related cell surface markers (i.e. CD73, CD90, CD105, SSEA-4), while being negative for hematopoietic cell markers. In addition to their regenerative potential of GMSCs, these cells also have potent immunomodulatory properties. GMSCs can influence a variety of innate and adaptive immune cells activation and fate. Of particular note are macrophages, and mast cells, which have been suggested to play a pivotal role in feline tooth resorption [14]. Additionally, GMSCs have been shown to express toll-like receptors (TLRs), that can be upregulated in an inflammatory milieu, a significant finding in the context of TR as this starts right at the gingival sulcus, a highly active area in terms of the presence of inflammatory cells. TLRs have been found on the surface of MSCs and consequently TLR receptor ligands, including neighboring bacteria, could potentially negatively impact the immunomodulatory ability of dental MSCs however, this aspect is still poorly explored [15, 16]. Importantly, GMSCs may maintain gingival anti-inflammatory homeostasis through the activation of Tregs. Furthermore, it was previously documented, that GMSCs may enhance the differentiation and activity of Tregs17 and thus play a critical role in gingival anti-inflammatory activity.

The oral cavity is considered a pro-inflammatory microenvironment and is likely significant for residing GMSCs that may lose their so-called pro-regenerative potential leading to reduced or lack or regenerative response and disease progression. GMSCs have promising regenerative and immunomodulatory properties, are numerous and can be obtained via less invasive techniques [17]. In addition, GMSCs exhibit higher proliferation capacity in comparison to bone marrow-derived MSCs and umbilical cord-derived MSCs [18] and lower population doubling time indicating a higher expansion potential. GMSCs possess the ability to differentiate into osteoblast, chondroblast, and adipocytes; however, at the same time under special circumstances, they may give rise to unique neural crest cells (NCCs) changing their secretory profile, morphology, and function [19]. The unique ability of GMSCs for multipotent differentiation and secretory potential of variety of soluble bioactive factors makes them a promising tool for periodontal tissues regeneration including the gingiva.

The use of MSCs has historically focused on their regenerative therapeutic effects as replacement cells due to their multipotent capacities. However, extensive evidence supports their use as a potent immunomodulatory/anti-inflammatory treatment and pleiotropic agent. MSC secretomes contain many biological factors such as extracellular vesicle (EV)-dependent- and/or independent-growth factors, cytokines, hormones, miRNAs, and other bioactive soluble factors.

The pro-regenerative potential of GMSCs is associated partially with their anti-oxidative activity [20]. Additionally, loss of integrity due to dysregulation of MSCs metabolism has been recognized in several disorders [21]. Growing evidence suggests that MSCs have antioxidant effect, which in part explains their anti-inflammatory, cytoprotective properties and both soft tissue and bone regeneration potential [22]. Several studies demonstrate that MSCs are resistant to oxidative insult, and because of their ability to secrete free radical scavengers including SOD1, SOD2, or glutathione peroxidase (GPx), MSC may play a substantial role in the modulation of oxidative stress related to tissue damage [23]. This molecular phenomenon is mediated by mitochondrial biogenesis, dynamics, and bioenergetics which significantly modulate the oxidative-anti-oxidative axis. Mitochondrial dysfunction in mesenchymal stem cells (MSCs) has been shown to be involved in the progression of multiple inflammatory diseases and the cellular senescence that results significantly affects the quantity and quality of MSCs. Research supports that abundant oxidative stress significantly impairs MSC's anti-inflammatory and multilineage differentiation potential [24]. Impaired mitochondrial metabolism and dynamics strongly correspond to the limited pro-regenerative potential of MSCs negatively impacting their clinical

applicability; however, such data does not exist for tooth resorption in any species. Investigating GMSCs in tooth resorption can provide insights into this disease's cellular and molecular mechanisms. Additionally, GMSCs have been shown to regulate inflammation and immune response and promote tissue repair and regeneration. By studying GMSCs in health (HE) and TR, researchers can better understand the mechanisms contributing to tooth resorption and potentially develop new therapeutic strategies to prevent this disease.

This study aims to identify the molecular signature, morphology, proliferative and clonogenic potential of GMSCs isolated from the gingiva of healthy and tooth resorption-affected cats. Specifically, we characterized essential aspects of the cyto-physiological characteristics of healthy feline GMSCs to better understand the molecular mechanisms involved in the limitation of their stemness in the course of tooth resorption.

Materials and Methods

Gingiva Tissue Harvesting and GMSCs Isolation

Gingiva tissue adjacent to TR lesion from three cats (i.e., diagnosed by clinical and dental radiographic means) that were otherwise systemically healthy were collected during an extraction procedure with the owner informed consent. The immediate cause of the cats' visits to the clinic was the inflammation of the gums observed by the owners. On clinical examination, gingivitis was observed without faucitis and without inflammation of the oral vestibule mucosa. In the case of stage 4, localised, slight gingival hyperplasia was observed. The clinical trial was conducted before the cats were premedicated.

In addition, gingiva obtained from teeth of healthy cats that were euthanized for reasons not related to this study were obtained immediately post-mortem. Gingival samples were obtained for cats in both groups and these were age (5–8 years old) and sex matched.

All steps involved in tissue isolation were performed under strictly sterile conditions using an enzymatic-mechanical method. Briefly, the gingiva was washed twice in sterile phosphate-buffered saline (PBS) containing 1% Penicillin–Streptomycin (PS) antibiotic mixture (Biowest, USA). The tissue was defragmented and incubated with collagenase I (Sigma-Aldrich, Poland) for 40 min in 37℃. Obtained cells were centrifuged (1500xg for 10 min) and washed with PBS. The isolated GMSCs were subsequently cultured in Dulbecco's Modified Eagle's Medium (DMEM) containing 1 g/L glucose, supplemented with 10% fetal bovine serum (FBS) and 1% penicillin–streptomycin antibiotic solution. Cells were grown in an incubator with 5% CO2 and 95% humidity at 37 °C. GMSCs from HE and TR-affected cats were seeded onto a 24-well plate at a density of 2.5×10^4 cells per well and left to attach for 24 h. Cells were passaged 3 times, then they were used for further studies [25].

Visualization of Cells' Mitochondria and Cytoskeleton

The morphology of healthy (fGMSC^HE) and diseased (fGMSC^TR) cells was evaluated with confocal microscopy. MitoRed dye (Sigma-Aldrich, cat. No 53271, Poland) was added to the culture medium (1:1000) and incubated for 30 min at 37 °C to visualize the mitochondrial network. Excess MitoRed was washed out using PBS prior to cell fixation in 4% PFA for 40 min at room temperature in the dark. For cytoskeleton visualization, cells from both groups were fixed in cold 4% PFA for 20 min at room temperature and permeabilized in a 0.1% Triton X-100 solution (Sigma-Aldrich, cat. No 93443, Poland) for 15 min. Actin filaments were then stained using atto-488-labeled phalloidin (Sigma-Aldrich, cat. No 49409, Poland) (1:800 in PBS) for 45 min, in the dark at room temperature. The nuclei were counterstained with DAPI (Faramount Aq Mounting Medium, Dako). The cells were observed and imaged using a confocal microscope (Observer Z1 Confocal Spinning Disc V.2 Zeiss).

Immunofluorescence Staining

fGMSC^HE and fGMSC^TR cells were seeded on cover slides as previously described. Then, the medium was removed, and cells were fixed with cold 4% PFA for 20 min and permeabilized in a 0.1% Triton X-100 solution for 15 min at room temperature. Cells were then incubated overnight with the primary antibodies (Table 1) diluted in 10% Normal Goat Serum in PBS. After that, the cells were incubated with Atto-594 secondary antibody diluted in PBS (1: 1000, Sigma-Aldrich, Poland) (Table 2). Cell nuclei were stained with DAPI (Faramount Aq Mounting Medium, Dako) or with Hoechst33342 (Sigma-Aldrich, Poland) (1:1000 in PBS) for 10 min in room temperature. Pictures were taken with a confocal microscope (Observer Z1 Confocal Spinning Disc V.2 Zeiss).

Proliferation Rate Assay

For the clonogenic assay, fGMSC^HE and fGMSC^TR cells were seeded in a 6-well plate at an initial density of 1×10^2 cells per well. After 7 days, cells were fixed in cold 4% PFA for 20 min at room temperature and stained for 5 min with

Table 1 Animal characteristics

Case number	Breed	Sex (neuter status)	Age	Body weight (kg)	Teeth affected by TR[a] (stage of disease or cause of death)
1	Europeian shorthair	Female (intact)	8	3,6	202 (4), 207 (2), 107 (3), 309 (1), 304 (2), 403 (3)
2	British shorthair	female (castrated)	7	3,3	303 (1), 202 (2), 203 (2), 103 (2), 409 (4a), 407 (1), 309 (1), 108 (3)
3	Ragdoll	female (castrated)	6	3,9	106 (1), 108 (1), 206 (1), 207 (1), 307 (1), 407 (3)
4	Europeian shorthair	Female (castrated)	5	4	CONTROL (traffic accident)
5	British shorthair	female (castrated)	6	4,5	CONTROL (HCM[b])
6	Europeian shorthair	female (castrated)	8	3,2	CONTROL (adenocarcinoma)

[a]-Modified Triadan System [26]

[b]-HCM – hypertrophic cardiomyopathy

Table 2 List of antibodies used for immunofluorescence

Antibodies	Concentrations	CAT numbers	Company
KI-67	1:1000	orb10033	Biorbyt
IL-1β	1:500	ab9722	Abcam
IL-10	1:500	DF6894	Affinity Biosciences

IL-1β Interleukin 1β; *IL-10* Interleukin 10

pararosaniline solution (Sigma-Aldrich, cat. No P3750, Poland). Colonies containing more than 50 cells were counted and colony forming (CFU) rate was obtained using the formula described by Kornicka K. et al. [21].

An expansion test was performed to evaluate cell migration capacity for both fGMSC[HE] and fGMSC[TR]. For this purpose, two groups of cells were seeded on 24-well plates as described above. After achieving 90% of confluency, a monolayer scratching test was performed. A series of photomicrographs were taken at 0 h, 6 h and 24 h. Cell migration parameters were analyzed using GraphPad Prism8 Software (San Diego, USA).

Senescence β-Galactosidase Staining

Detection of aging-related lysosomal enzyme (SA-β-Gal) was performed with Senescence Cells Histochemical Staining Kit (Sigma-Aldrich, Poland) according to the manufacturer's instructions. Briefly, fGMSC[HE] and fGMSC[TR] cells were fixed by incubation for 6 min with 1×Fixation Buffer (1:10 in PBS). The buffer was changed to Staining Mixture, containing Staining Solution 10x, Reagent B, Reagent C, X-gal Solution, and ultrapure water. Cells were incubated at 37 °C for 48 h in the incubator without CO_2, and subsequently observed using an invert microscope (Leica, Germany). Obtained results were

analyzed with ImageJ Software and GraphPadPrism8 Software (San Diego, USA).

Gene Expression Analysis

Total RNA was isolated from fGMSC[HE] and fGMSC[TR] cells with EXTRAzol reagent (Blirt, Poland) following the manufacturer's instructions. The concentration, quality and purity of isolated RNA was verified with a nanospectrophotometer (Epoch, BioTek). Transcription of RNA into cDNA was performed using the Takara PrimeScriptTM RT Reagent Kit with gDNA Eraser (Perfect Real Time) according to the manufacturer's protocol. A real-time polymerase chain reaction (qPCR) was performed using the SensiFast SYBR & Fluorescein Kit (Bioline, London, UK) and a CFX ConnectTM Real-Time PCR Detection System (Bio-Rad, Poland). Each reaction amplified 150 ng of cDNA in a final volume of 10 μl. The thermal cycling conditions were as follows: 95 °C for 2 min followed by 41 cycles at 95 °C for 15 s, annealing for 30 s and elongation at 72 °C for 15 s. The RT-qPCR reaction was performed at least in three repetitions. The relative expression levels of each targeted gene (Tables 3 and 4) were normalized in relation to the expression of the glyceraldehyde 3-phosphate dehydrogenase (GAPDH) using the 2-ΔΔCq method.

To conduct RT-qPCR for miRNA, the Mir-X miRNA First Strand Synthesis Kit (Takara, Sweden) were used. Briefly, gDNA traces were removed by treating the RNA with the Dnase I, Rnase-free in 10X reaction buffer with MgCl2 and water, at 37 °C for 30 min. The volume of obtained RNA (1000 ng/ul), was mixed with mRQBuffer (2X) and mRQEnzyme. The reaction mixture was incubated at 37 °C for 1 h, then at 85 °C for 5 min. The expression level of miRNA was analyzed by Real-Time PCR using the MicroRNA first-strand synthesis kit (Takara,

Table 3 Sequences of primers used in qPCR

Gene	Primer Sequence (5'->3')
CD44	F: ACTGATGGCAAAGGTGGAAG
	R: TTGTGTGCCCAGCTGATTCT
CD45	F: GGCATTTGGCTTTGCCTTTC
	R: TAAGACTCTGATCAGGACTGGAA
CD73	F: AACCTGATTTGTGATGCCA
	R: TAATTGTGCCGTTGTTCCG
CD90	F: CTGCAGCAGCAGAGGACG
	R: GGGGTTCATGGTGCAGAGAG
BAX	F: TCTCCCCGTGAGGTCTTCTT
	R: CGCTCTCGAAGGAAGTCCAG
BCL2	F: AACCGGGAGATCGTGATGAA
	R: ATGGGCCTTAGTGGCGATGT
p21	F: GAGACGGTGGCTTGGAGAG
	R: CACCTGCAGCTCCTCCG
p53	F: GCTTCCCAGGACGGTGAC
	R: GGCTCGATGGTGAGTTCCAA
KI-67	F: GGTCGTCTGAAACCGGAGTT
	R: CTGGGGTTGTGTGGTCACTT
mTOR	F: CAACCCGATGGCCAGCATTA
	R: GGGGTCATCCTTGTTCGTGT
c-MYC	F: TGCTGAGTTGGACAGTCGTC
	R: AGTAGTCAGCAACACGAGGC
HSP60	F: AGCCCGGGAACTAGCCTAA
	R: AGCATTAAGGCTCGGGCATC
TFAM	F: GACTGCGCTCTCCTTTCAGT
	R: AGTTCCCTCCAAAGTTGGGC
FIS1	F: GCACGCAGTTTGAGTATGCC
	R: CTTGAGCCGGTAATTCCCCA
PINK1	F: AGGAACTCGTCCCAGCTAGT
	R: TGGCAGCAGTGGTACAGAAG
MFN1	F: AGTTGTCTTTAATTGCCCGTCT
	R: TGATCAAGTTCTGGATTCCTGT
MFN2	F: ACGCGATGTCCCTGCT
	R: TTCCGCATTCCTGTAGGTGT
SOD1	F: TTGGAGACCTGGGCAATGTG
	R: CGGCGTTTCCTGTCTGTGTA
SOD2	F: CGCTGGAGAAGGGTGACATT
	R: CACGTTTGATGGCTTCCAGC
CAT	F: TCGAGTGGCCAACTACCAAC
	R: TAGAAGGTCCGCACCTGAGT
NOS1	F: GATTAGTGCCGCTGGCCTC
	R: TGGCTGCGTCTAGATGTGTC
TXN1	F: CCGCCCCCAGTCGCTATAA
	R: ATCCCCAGCACTGTTCAAGG
NRF2	F: CCCCGCAGGTTTCTTAAGCC
	R: GTAGGCAGGCGATAGCTGTT
IL1α	F: TGCTACTGATCTGGGCTTCAT
	R: TCACCAGCACCTTTGTCCAC
IL4	F: GCAGCTCTGCAGAAGATTTCC
	R: CGGTCTTGTGGAGTTTCAGC

Table 3 (continued)

Gene	Primer Sequence (5'->3')
IL6	F: CTGCGACTGCAAGATAGCCT
	R: CACCCTACTTGAGGACGACTG
IL10	F: GGATCATCTCCGACAGGGC
	R: TGCTACTGATCTGGGCTTCAT
TGFβ	F: CAAGAAAAGTCCGCACAGCA
	R: CTGAGGTAGCGCCAGGAATC
TNFα	F: GCTGCACTTTGGAGTGATCG
	R: CCCTCAGCTTCGGGGTTTG
GAPDH	F: GATTGTCAGCAATGCCTCCT
	R: GTGGAAGCAGGGATGATGTT

CD44, CD45, CD73, CD40: Surface markers; BAX: BCL-2-associated X protein; BCL-2: B-cell lymphoma 2; p21: cyclin-dependent kinase inhibitor 1A; p53: tumor suppressor p53; KI-67: Marker Of Proliferation Ki-67; mTOR: mammalian Target of Rapamycin; c-MYC: cellular Myc; HSP60: heat shock proteins 60 kDa; TFAM: Transcription Factor A, Mitochondrial; IL1α: Interleukin 1α; IL4: Interleukin 4: IL6: Interleukin 6; IL10: Interleukin 10; TNFα: Tumor necrosis factor; TGFβ: Transforming growth factor beta; SOD1: Superoxide dismutase [Cu–Zn]; SOD2: Superoxide dismutase [Mn]; CAT: Catalase; NOS1: Nitric Oxide Synthase 1; TXN1: Thioredoxin1; NRF2: nuclear factor erythroid 2–related factor 2; FIS1: Mitochondrial fission 1 protein; MFN1: Mitofusin-1; MFN-2: Mitofusin-2; PINK1: PTEN Induced Kinase 1; GAPDH: Glyceraldehyde 3-phosphate dehydrogenase;

Table 4 Sequences of microRNA primers used in qPCR

Primer miRNAs	Primer Sequence (5'->3')
miR155	TTAATGCTAATCGTGATAGGGGTT
miR146	TGAGAACTGAATTCCATGGGTT
miR17-5p	CAAAGTGCTTACAGTGCAGGTAG
miR101-1/2	TACAGTACTGTGATAACTGAA
miR378	ACTGGACTTGGAGTCAGAAGG

cat. No. 638315, Sweden) according to the instructions provided by the manufacturer. Briefly, the reaction mixture contained water, SensiFast SYBR & Fluorescein Kit (Bioline, London, UK), miRNA-specific primer (Table 3), mRQ 3'primer, and cDNA. As a reference sample, U6F primer and U6R primer were used. The relative expression level was calculated by comparison of the tested groups with the control group using the 2-ΔΔCq method [27, 28].

Microcapillary Cytometry

Cell metabolism was evaluated with microcapillary cytometry using Muse ™ Cell Analyzer (Merck, Germany) in fGMSC^{HE} and fGMSC^{TR} cells. The level of oxidative stress and apoptosis in the cell was analyzed with commercially available kits according to the instructions

provided by the manufacturer. To determine the content of reactive oxygen species in the cell, Muse® Oxidative Stress analysis (Luminex) was used based on the manufacturer protocol. The cells were diluted into 1xAssay Buffer and incubated with Muse® Oxidative Stress working solution at 37 °C for 30 min. Then, cells were subjected to ROS analysis. The content of live and dead cells as well as the apoptosis of cells was analyzed using the Muse® Annexin V & Dead Cell Kit (Luminex). Cultured cells were incubated with Muse® Annexin V & Dead Cell Reagent (Luminex) at relative room temperature for 20 min and then examined using Muse ™ Cell Analyzer (Merck, Germany). In order to analyze mitochondrial potential, the Muse MitoPotential analysis (Luminex) was performed. Briefly, 90uL of MitoPotential Working Solution (1:1000 in $1 \times$ Assay Buffer; Luminex) was mixed with 100 ul cells (1×10^5 cells/tube) and incubated at 37℃ for 20 min. Then 5 ul of Muse®-7AAD reagent (Luminex) was added. After 5 min of incubation in RT, the mitochondrial potential was analyzed with Muse ™ Cell Analyzer (Merck, Germany). The obtained results were analyzed with GraphPad Software 8 (San Diego, USA).

Statistical Analysis

The data analyzed by one way variance analysis (ANOVA) using GraphPad Software 8 (San Diego, USA) and post-hoc Tukey's test. Statistically significant results were marked with a hashtag, for: $p < 0.05$ (#), $p < 0.01$ (##) and $p < 0.001$ (###) when comparing TR to HE. Results are presented as statistical mean SD from at least three independent experiments, with three technical repetitions.

Results

Identification of GMSCs Morphology and Growth Characteristics

The cell morphology was evaluated using confocal microscopy. To visualize nuclei, fGMSC^HE and fGMSC^TR cells were stained with DAPI whereas actin filaments were stained with phalloidin (PI), and mitochondria with MitoRed dye (Fig. 1A). GMSC from HE cats were characterized by uniform, bipolar, elongated, fibroblast-like shape, whereas GMSC from cats with TR possessed enlarged nuclei and a flat, irregular shape. In addition, RT-qPCR was used to assess surface markers of GMSCs. Isolated cells were characterized by the ability to express: CD44, CD 45, CD73, CD90 and s-100. Expression of CD44 (Fig. 1B) and CD45 (Fig. 1C) were increased in TR group compared to the GMSCs isolated from the HE group. CD73 was downregulated in TR (Fig. 1D) while

CD90 (Fig. 1E) showed no significant changes among the group. We also notice upregulation of s-100 in the GMSC cells isolated from affected cats (Fig. 1F). Furthermore, we evaluated the ability of cells to form colonies originating from single cells using the CFU-F assay. Hence, colonies were stained with pararosaniline and counted under a light microscope. The greatest number of colonies is clearly visible in the HE group. Moreover, data was quantified using a CFU-F algorithm, disclosing a lower ability to form colonies in TR when compared to HE cells (Fig. 1G). Using fluorescence microscopy, we visualized senescent cells in cultures using β-galactosidase staining. Quantification revealed an increased number of senescent cells in TR group (Fig. 1H). Using immunofluorescence staining, we then determined the expression of Ki-67 for evaluation of proliferation rate of isolated cells (Fig. 1I). Additionally, RT-qPCR was performed for obtaining relative gene expression for KI67 (Fig. 1J). Obtained data showed no significant differences between proliferation of TR and HE cells (Fig. 1I, J). To better understand the differences in proliferation, differentiation, growth, and survival between TR affected and healthy cells, we examined the expression levels of a key regulator of these processes, mTOR (mammalian target of rapamycin), using PCR reaction (Fig. 1H). Results showed decreased expression of *mTOR* gene in TR showing their impaired therapeutic potential. Using PCR, the expression of proliferation-related miRNA in isolated GMSC cells was established. Lower expression of miR-17 was noted in the TR group compared to the HE group (Fig. 1L). No differences in expression of miR-101 (Fig. 1M) and miR-17 (Fig. 1L) were noted between groups. Interestingly, miR-378 was found to be up-regulated in TR (Fig. 1N). Finally, we performed an expansion assay to support obtained results. Quantification data showed that the ability of cell migration was significantly reduced in TR compared to the HE (Fig. 1O). These results together suggest that GMSCs isolated from affected cats have deteriorated functionality caused by impaired proliferation and growth.

Assessment of Apoptosis Factors

RT-qPCR was performed to determine expression levels for apoptosis related genes. The apoptotic incidence in TR demonstrated a significantly higher expression in comparison to the HE group. We also noticed the expression levels of mRNA's coding proapoptotic proteins p53 (Fig. 2A) and p21 (Fig. 2B) were significantly enhanced in cells from the TR group compared to the HE group. A similar phenomenon was observed for the expression levels of the cell cycle regulator C-MYC (Fig. 2C). Relative expression of BCL-2 was downregulated in TR (Fig. 2D) and BAX was upregulated in that group as compared to the HE group
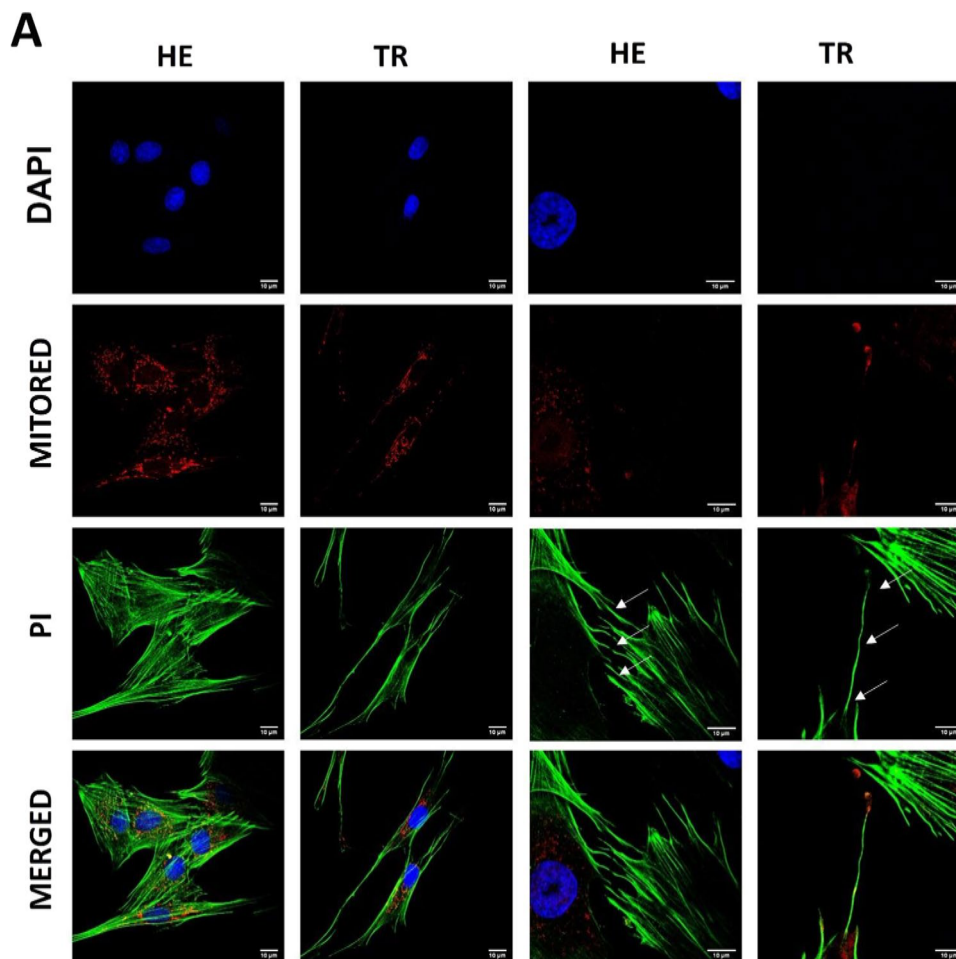
Fig. 1 Growth characteristics and morphology of GMSCs. Cells were cultured for 24 h and subjected to further analysis. Staining for nuclei (DAPI), mitochondria (mitoRed dye) and f-actin (Phalloidin) revealed that some cells in TR were characterized by enlarged nuclei and flat, spread-out cell body with visible stress fibers (white arrows) (Fig. 1A). RT-qPCR results demonstrate the expression of the following surface markers CD44 (Fig. 1B), CD45 (Fig. 1C), CD73 (Fig. 1D), CD90 (Fig. 1E), and s-100 (Fig. 1F). The ability of cells to form colonies originating from one cell was evaluated by CFU-F assay. Representative photographs showing colonies stained with pararosaniline and quantitative data obtained by the application of a CFU-F algorithm are shown (Fig. 1G). Representative photographs showing the results of senescence-associated β-galactosidase staining with quantities graphs (Fig. 1H). Ki67 staining established proliferation abilities of cells that were observed under confocal microscope (Fig. 1I). Growth and proliferation characteristics were also examined with RT-qPCR for KI67 (Fig. 1J), mTOR (Fig. 1K) and miRNA's including miR-17 (Fig. 1L), miR-101 (Fig. 1 M), miR-378 (Fig. 1N). Proliferation rate and healing properties of GMSCc were also assessed by performing expansion assay and observing cells under light microscope after 0, 6 and 24 h. Representative photographs and quantitative data are presented (Fig. 1O). Results are expressed as mean ± SD; $n = 3$. #$p < 0.05$, ##$p < 0.01$, and ###$p < 0.001$

(Fig. 2E). The pro-apoptotic gene expression pattern for cells from the TR group was shown by an elevated BAX/BCL-2 ratio (Fig. 2F). To support these findings, we used Muse® Annexin V (Fig. 2G) to determine the proportion of viable cells versus cells undergoing apoptosis. The TR group showed a significantly reduced number of live cells (Fig. 2H) and an increased number of early apoptotic cells compared to HE (Fig. 2I). Additionally, we observed a slightly increased percentage of dead cells in the TR group (Fig. 2J) as well as reduced late apoptotic/dead ratio compared to HE (Fig. 2K). Apoptosis profile analysis supported the results indicating lower viability of GMSC cells derived from TR affected patients.

Inflammation

To further investigate the molecular changes between GMSCs isolated from HE and TR affected patients we evaluated the most common inflammatory related genes via RT-PCR analysis. Results showed significantly increased expression levels of IL-1a (Fig. 3A), IL-6 (Fig. 3B), TNF-α (Fig. 3C) and IL-4 (Fig. 3E) in the TR group. Importantly, IL-4 was also up-regulated in TR (Fig. 3E). For the IL-10 we observed significantly lower expression levels in TR compared to the HE (Fig. 3F). Expression of TGF-β did not show significant differences
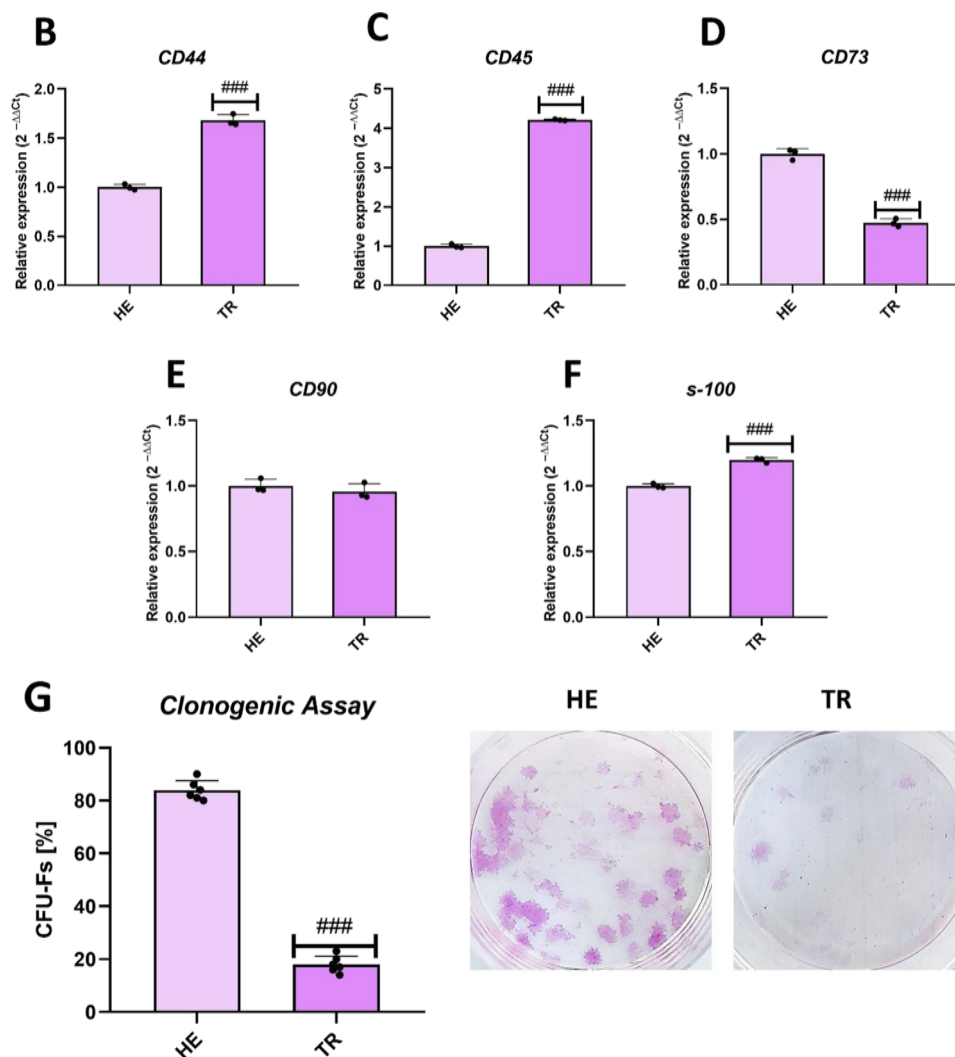
B *CD44*

C *CD45*

D *CD73*

E *CD90*

F *s-100*

G Clonogenic Assay

HE   TR

Fig. 1 (continued)

between groups (Fig. 3G). Meanwhile, the RT-PCR analysis for miR-155 (Fig. 3D) and miR-146 (Fig. 3H) demonstrated significantly increased expression in TR. Furthermore, immunofluorescence staining for IL-1b (Fig. 3I) and IL-10 (Fig. 3J) confirmed RT-PCR results.

Oxidative Stress and Mitochondria

Mitochondrial dynamics were assessed by RT-PCR via investigation of expression of HSP60, TFAM, FIS1, PINK1, MFN1 and MFN2 genes. This analysis showed important differences between groups. The expression of HSP60 (Fig. 4A) was upregulated in the HE group whereas the expression of TFAM (Fig. 4B) and mitochondrial fission promotor FIS1 (Fig. 4C) were upregulated in the TR group. Evaluation of the relative expression of another major marker related to selective mitophagy and mitochondrial dynamics and biogenesis— PINK1, showed this marker to be significantly diminished in

TR (Fig. 4D). Mitochondrial fusion-related factors, such as MFN1 (Fig. 4E) was elevated in the TR group and MFN2 (Fig. 4F) was downregulated in this group. Moreover, we performed RT-PCR to test the antioxidative properties of the investigated cells by analyzing expressions of SOD1, SOD2, CAT, NOS1, TXN1 and NRF2. Interestingly, both SOD1 (Fig. 4G) and SOD2 (Fig. 4H) showed enhanced expression in TR group. The expression levels of CAT showed no significant differences between groups (Fig. 4I). On the other hand, mRNA expression levels of NOS1 were augmented in TR (Fig. 4J) and there is significant upregulation of TXN1 (Fig. 4K) and NRF2 in TR compared to HE (Fig. 4L). Furthermore, mitochondrial membrane potential was established with a MUSE cell analyzer (Fig. 4M) and the data was quantified. There was no significant difference in the number of live cells between HE and TR and depolarized/live ratio. However, results showed an increased number of depolarized/dead cells and total dead cells in TR compared to HE. Mitochondrial impairment is hallmarked by excessive
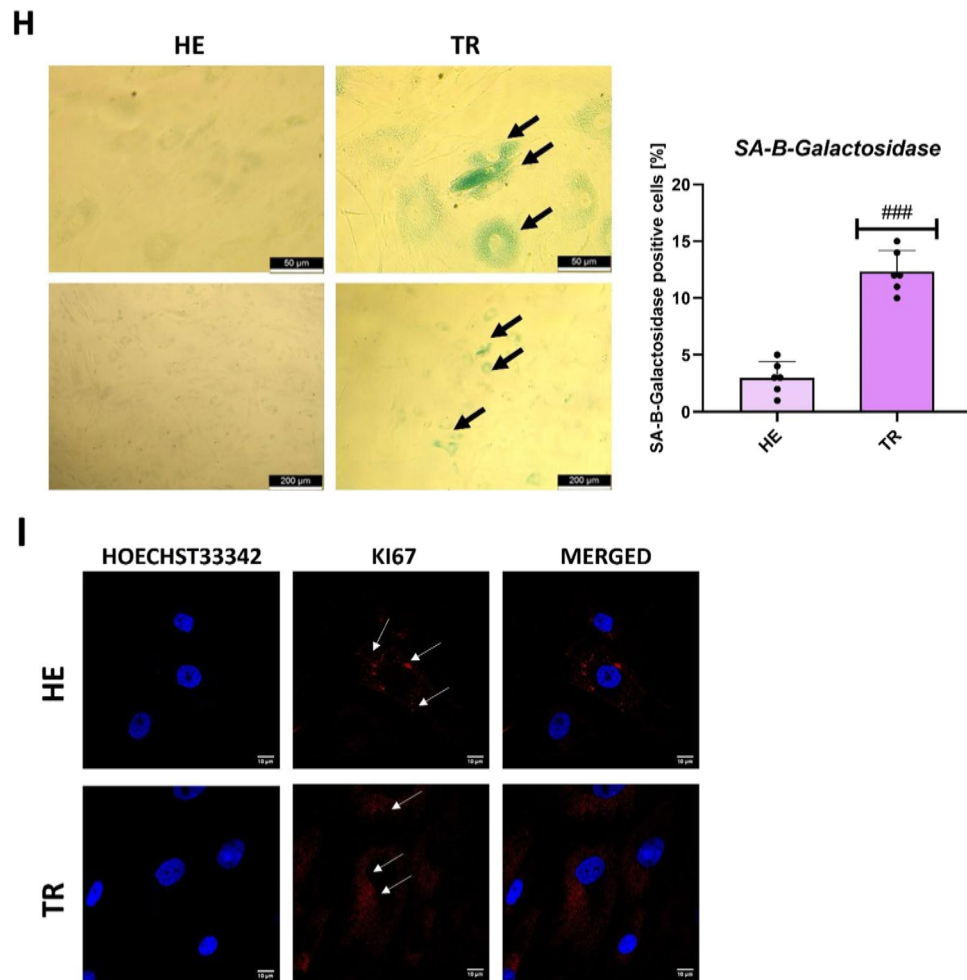
Fig. 1 (continued)

ROS accumulation leading to global metabolic failure and therapeutic potential disturbance. Therefore, to determent the oxidative status of these cells, we measured the accumulation of ROS by flow cytometry using Muse® Oxidative Stress assay (Fig. 4N). Our results displayed that fGMSC^{TR} is characterized by increased negative ROS accumulation.

Discussion

Interest in the use of MSCs in clinical practice is on a trajectory due to their immunomodulatory effect and regenerative potential [29–32]. However, their involvement in the pathophysiology of oral diseases still remains largely elusive.

This study isolated and characterized fGMSCs in HE as well as TR affected cats. We found several important findings indicating limited stemness of fGMSC^{TR}, expressed by deteriorated morphology, limited proliferative and expansion potential, and enhanced senescence as well as

apoptosis. Moreover, we noted, that fGMSC^{TR} exhibit an elevated expression of pro-inflammatory markers with concurrent reduced activity of anti-inflammatory cytokines at an mRNA and protein level. Finally, we found that fGMSC^{TR} secret a higher amount of ROS potentially caused by impairment of mitochondrial fission and fusion.

We found that fGMSC^{TR} present a unipolar morphotype with densely located mitochondria on one side of the cells which partially explains their limited expansion and clonogenic potential. [33] In contrast, fGMSC^{HE} were characterized by spindle shape morphotypes with densely located mitochondria around nuclei as was observed in another study investigating human GMSCs [34, 35] We also found that patients affected with TR expressed higher CD44 and CD45 and at the same time exhibited a lower expression of CD73 which can have implications in their immunomodulatory potential. Decreased expression of CD45 marker may indicate a reduced ability of fGMSC^{TR} for promotion of angiogenesis [36] (ref. https://pubmed.ncbi.nlm.nih.gov/26309784/), which could be a critical component in the
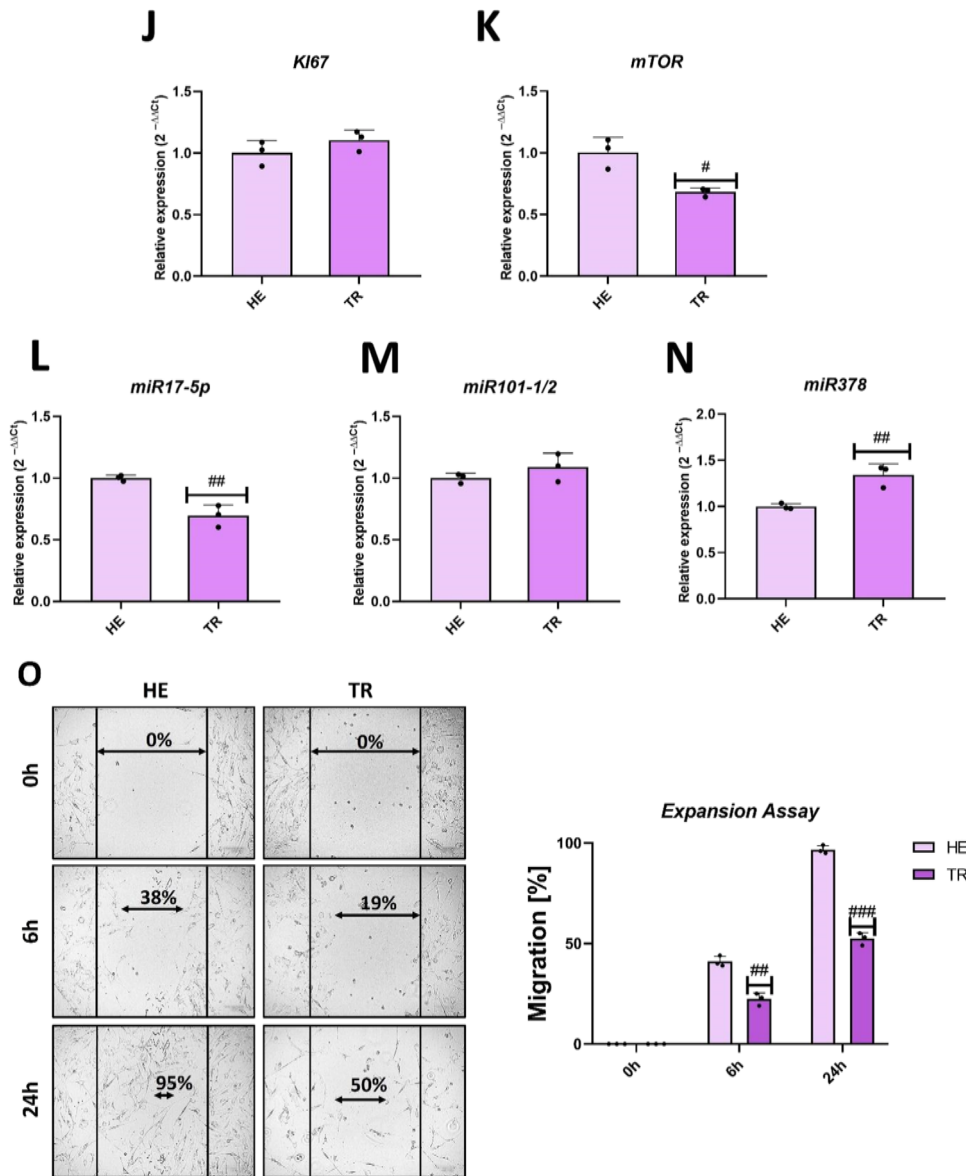
Fig. 1 (continued)

course of TR. Observed changes in fGMSC^{TR} morphology and surface marker expression might become a valuable future parameter allowing to select a proper MSCs morphotype for cell based treatments.

Proliferative and clonogenic potential as well as expansion capability and viability are cardinal features of stromal cells that affect their stemness and consequently regulate their pro-regenerative potential. GMSCs have been suggested to have the potential to regenerate damaged dental tissues [37, 38] (https://doi.org/10.3390/cells8060537, https://doi.org/10.3892/mmr.2016.5726). By investigating GMSCs in tooth resorption, researchers can explore the regenerative potential of these cells and identify ways to enhance their regenerative capacity. In addition, GMSCs can

be isolated from an individual's gingival tissue, making them a potential source of personalized cell-based therapy for tooth resorption. Investigating GMSCs in tooth resorption can help identify the best approaches for isolating and expanding these cells and determine the optimal dosing and delivery methods for personalized treatment.

Here we showed, that fGMSC^{HE} exhibits greater expansion and proliferative potential while presenting reduced senescence markers and more stable surface receptors expression related to stemness, suggesting healing and new tissue formation capabilities. This is in line with findings from comparative studies which have shown that the migration potential of periodontal derived MSCs corresponds with their wound healing and periodontal regeneration potential

Fig. 2 Differences in apoptotic propensity between GMSCc isolated from healthy and infected patients. Key apoptotic markers were evaluated via RT-qPCR. Bar charts are illustrating the relative expression of major apoptotic markers including p53 (Fig. 2A), p21 (Fig. 2B), c-MYC (Fig. 2C), BCL2 (Fig. 2D), BAX (Fig. 2E), and BAX:BCL2 ratio (Fig. 2F). The Muse® Annexin V & Dead Cell assay was used to assess live cells, early and late apoptotic cells, as well as dead cells (Fig. 2G). According to the Muse® Annexin V & Dead Cell assay, histograms reflect the ratio of live (Fig. 2H), early apoptotic (Fig. 2I), late apoptotic (Fig. 2J), and dead cells (Fig. 2K). Results are expressed as mean $\pm$ SD; $n = 3$. $\#p < 0.05$, $\#\#p < 0.01$, and $\#\#\#p < 0.001$
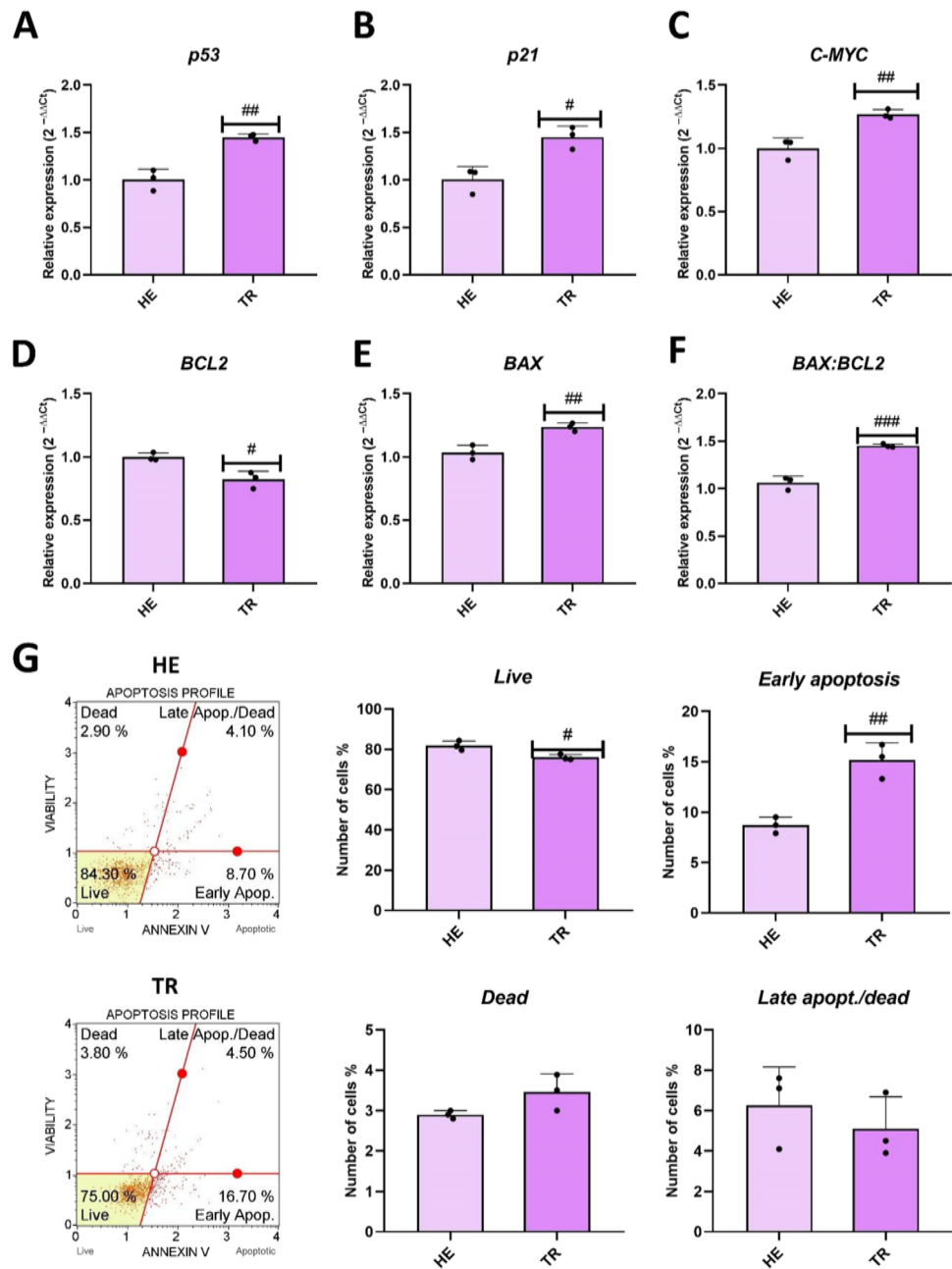
while allowing for minimal scar tissue formation [39]. On the other hand enhanced senescence as seen in the fGMSC^{TR} of this study may lead to a reduction of MSCs multilineage differentiation potential and new bone formation as has been previously suggested in the literature [17, 40] thereby questioning their potential application for bone regeneration. In the future, the multilineage differentiation potential of GMSCs from HE as well as TR affected patients should be assessed to determine their osteogenic potential.

Due to their unique properties stromal cells are commonly used in veterinary regenerative medicine; however, as shown by our and other research groups' findings,

diseases can alter their pro-regenerative potential [41]. Our results regarding fGMSC^{TR} partly contradict previous studies that evaluated the effects of other dental diseases on human GMSCs where results showed that disease did not result in impaired regenerative properties. On the one hand a study evaluating GMSCs in individuals affected by periodontal disease showed no change in surface marker expression and an increased osteogenic capability due to the overexpression of several proinflammatory cytokine-dependent chaperones and stress response proteins [42]. On the other hand, GMSC have also been isolated from sites affected by gingival hyperplasia showing that both
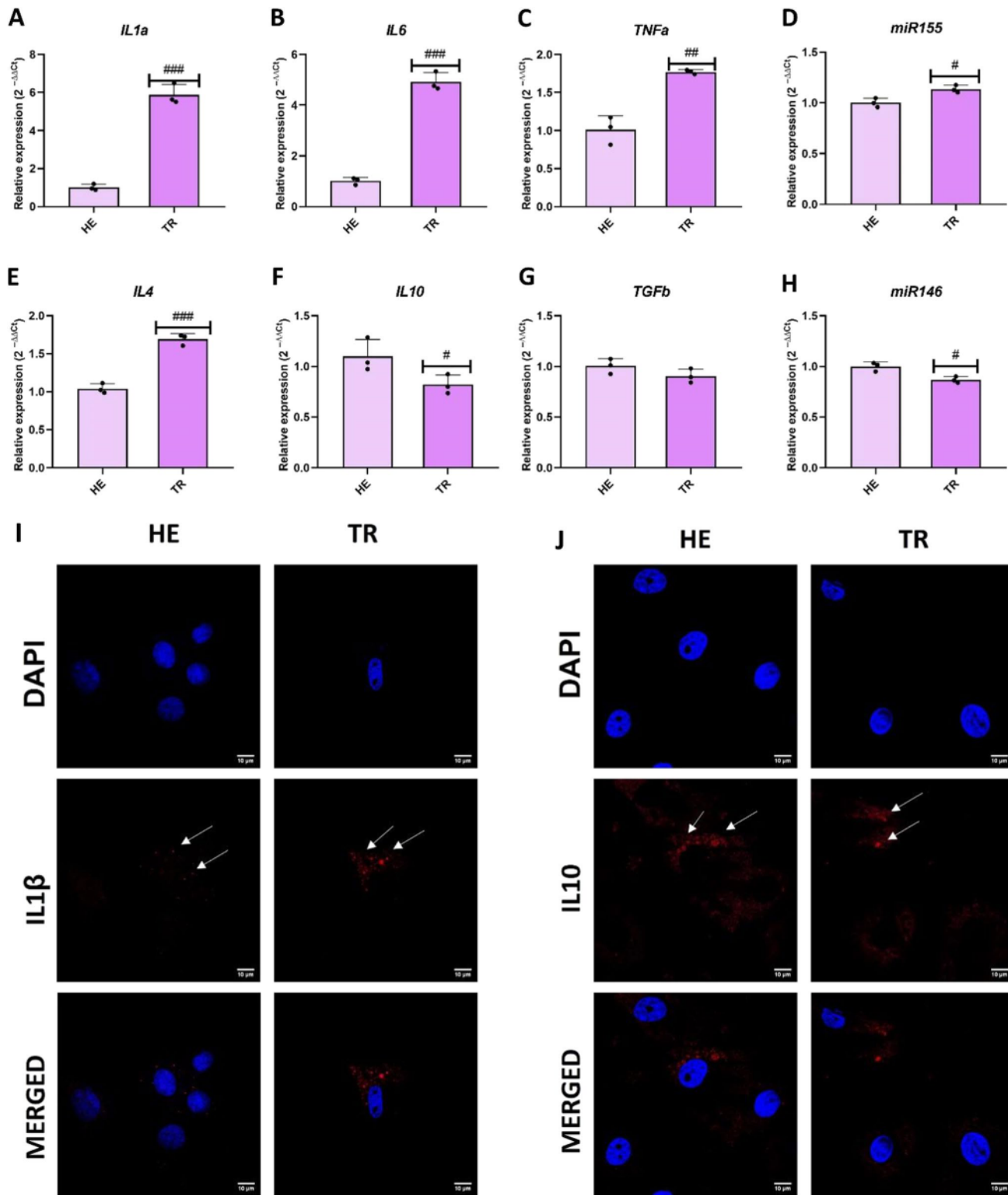
Fig. 3 Evaluation of inflammation. Using RT-PCR, the expression of IL1α (Fig. 3A), IL6 (Fig. 3B), TNFα (Fig. 3C), miR155 (Fig. 3D), IL4 (Fig. 3E), IL10 (Fig. 3F), TGFβ (Fig. 3G), miR146 (Fig. 3H) was assessed in GMSCS. Furthermore, localization of IL1β (Fig. 3I) and IL10 (Fig. 3J) was assessed using immunofluorescence. Results are expressed as mean ± SD; $n=3$. #$p<0.05$, ##$p<0.01$, and ###$p<0.001$
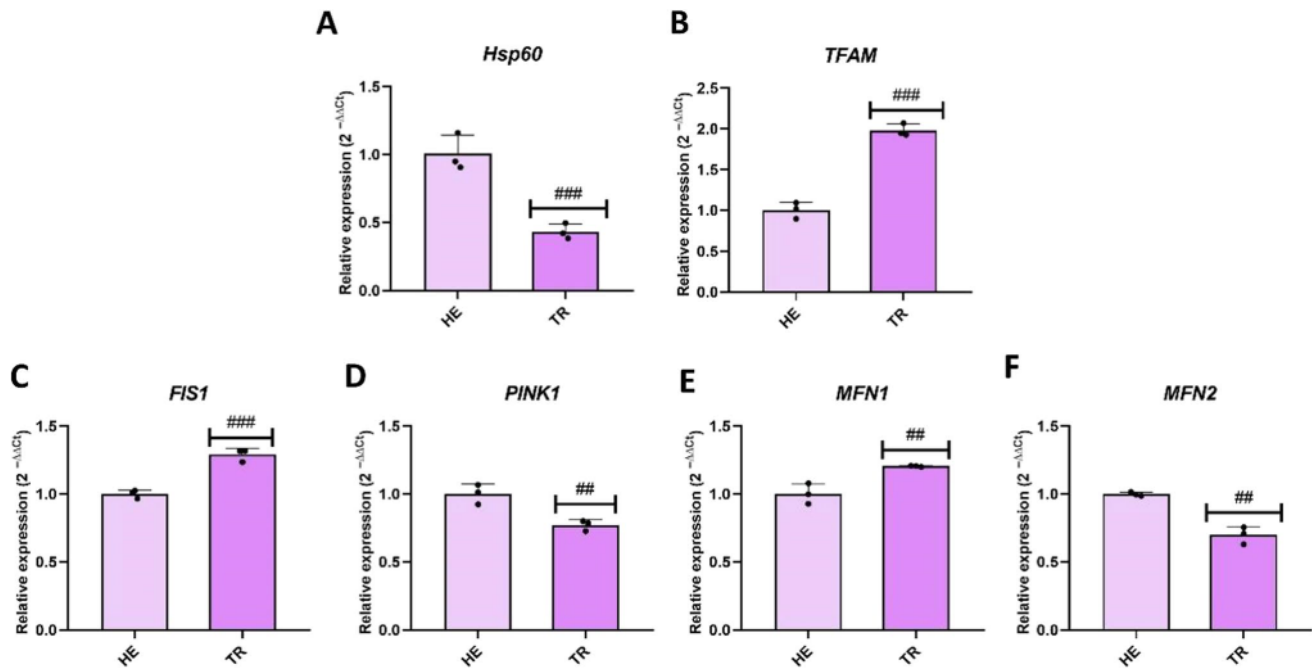
Fig. 4 Mitochondrial dynamics and oxidative stress in GMSC cells. Representative bands show the results of RT-qPCR analysis for key mitochondrial dynamics markers as Hsp60 (Fig. 4A), TFAM (Fig. 4B), FIS1 (Fig. 4C), PINK1 (Fig. 4D), MFN1 (Fig. 4E), MFN2 (Fig. 4F), SOD1 (Fig. 4G), SOD2 (Fig. 4H), CAT (Fig. 4I), NOS1 (Fig. 4J), TXN1 (Fig. 4K), and NRF2 (Fig. 4L). For further investigation of mitochondrial membrane potential (MMP) flow cyto-metric analysis was performed (Fig. 4 M). Percentage of total live, depolarized/lived, depolarized/dead and dead are shown. Oxidative stress was established also with the use of flow cytometry (Fig. 4N). The plots show ROS positive and ROS negative percentage of cells among the HE and TR. Results are expressed as mean $\pm$ SD; $n = 3$. #$p < 0.05$, ##$p < 0.01$, and ###$p < 0.001$

GMSC from healthy as well as hyperplastic gingiva possess self-renewal and multipotent differentiation properties. Notably in that study, GMSC from hyperplastic tissues exhibited a more robust regenerative capability suggesting that these cells perhaps have a role in the development of the hyperplastic phenotype [43]. In addition to the already mentioned altered properties the present study also found that TR induced expression of components of the p21-p53 axis. To the author's knowledge no study so far has isolated and characterized GMSCs from TR or HE sites and further demonstrate that GMSCs isolated from TR areas do display altered regenerative potential.

To evaluate fGMSCs immunomodulatory potential, we analyzed their ability to secrete pro and anti-inflammatory cytokines and we found that fGMSC[HE] abundantly secrete anti-inflammatory cytokine, Il-10. This is in line with findings from comparative studies demonstrating that GMSCs secrete reduced amounts of TNF-α together with enhanced release of IL-10 and therefore may substantially modulate the anti-inflammatory microenvironment of the gingiva contributing to tissue regeneration [15]. Consequently, fGMSC[HE] should be further evaluated as a novel treatment option for periodontal disease in cats. The opposite holds true for fGMSC[TR] cells due to the lower expression of CD73 that was noted. CD73 is a critical marker for the modulation of Tregs associated anti-inflammatory state [44] thus this finding may have an implication on the homeostatitc balance between Tregs and CD8 lymphocytes in TR sites.

MSCs also participate in tissue homeostasis, remodeling, and repair by ensuring the replacement of mature cells during physiological turnover in addition to injury or disease [45]. The present study demonstrated a state of GMSC dysfunction in patients with TR.

Tooth resorption is a clinically progressive disease. In the absence of a better understanding of its cause, the effects continue to be devastating to the patient's teeth. In cats as well as humans, this condition may lead to tooth loss and a feeling of helplessness by clinicians, pet owners, and patients due to a lack of effective prevention/treatment options that will allow for the preservation of teeth and the achievement of a cure. Furthermore, in humans, the resultant poor esthetics and function may negatively impact mental health and wellbeing [46]. Altered periodontal structures and microenvironment have been proposed as contributing factors of TR [47, 48] yet the factors that activate osteoclasts/odontoclasts and draw them to root surfaces remain unknown. Our study found that fGMSCTR create
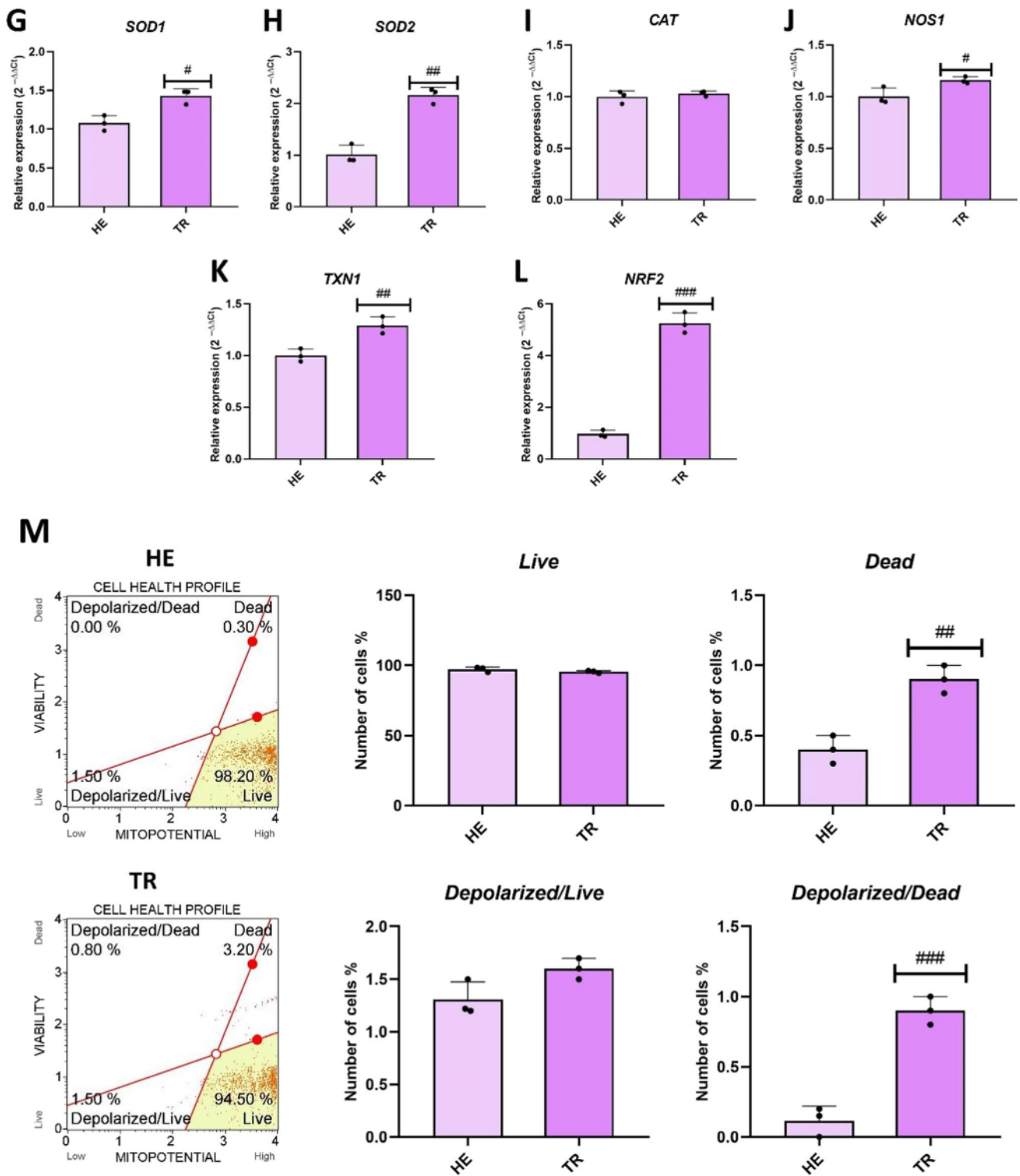
Fig. 4 (continued)

a pro/anti-inflammatory environment by releasing various cytokines and specific microRNA, including miR-155, miR-17, and miR-378. fGMSCTR in this study highly expressed miR-155, a known biomarker of periodontal diseases in humans.49 Studies have shown that elevated expression of miR-155 in patients with periodontal disease was positively correlated with the severity of the clinical parameters of periodontal diseases [49]. In turn, decreased expression of
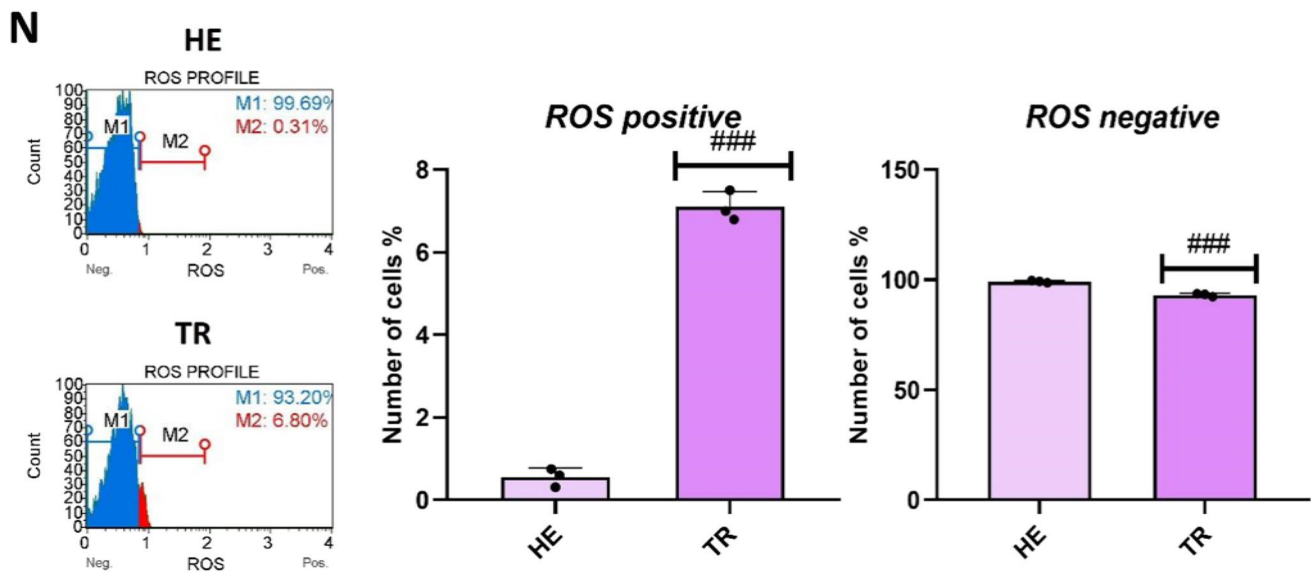
Fig. 4 (continued)

miR-17 mitigates the inflammatory microenvironment and promotes an anti-inflammatory phenotype of the progenitor cells. Moreover, miR-378 influences mesenchymal stem cell phenotype and function with the promotion of adipose stem cell (ASCs) differentiation potential, and IL-4 induces miR-378 and therefore is recognized as a key player involved in macrophage cytokine production. Moreover, we have identified a higher ROS accumulation in fGMSCTR and enhanced mitochondrial membrane depolarization. Observed reduced anti-oxidative potential of fGMSCTR can contribute to increased oxidative stress state in the periodontium and abundant ROS secretion potentially due to mitochondrial failure, thereby aggravating the periodontal injury [50].

Deterioration of mitochondrial dynamics in fGMSC^{TR} is likely playing a role in feline TR. We demonstrated decreased expression of Fis1 and Mfn2 in GMSCs isolated from fGMSC^{TR} patients which might indicate a link between mitochondrial dynamics and reduced stemness and expansion properties. Similar observations have been made by Wang et al., who showed abnormal mitochondrial structure and function in human gingival tissue of patients with chronic periodontitis [51]. Moreover, impaired mitochondrial dynamics might be one of the reasons explaining reduced immunomodulatory potential of fGMSC^{TR}. Recent studies show that defective mitochondrial dynamics inhibits mitochondrial transfer for Tregs and thus promotes pro-inflammatory gingival microenvironment in periodontal diseases [52]. Future studies should focus on the effects of GMSC from TR in terms of their multilineage differentiation potential especially in co-culture with osteoclast to identify their osteogenic/osteoclastogenic regulatory potential and to verify whether mitochondrial replacement in

deteriorated cells might be an potential strategy to restore their stemness and become a future therapeutic tool.

Conclusion

The present study isolated and characterized fGMSC^{HE} and fGMSC^{TR} affected sites. We demonstrated that fGMSC^{HE} exhibit enhanced clonogenic potential and have a unique ability to modulate the gingival microenvironment through the induction of the activity of critically important anti-inflammatory cytokines. Conversely, fGMSC^{TR} have impaired regenerative and immunomodulatory properties. These cells may contribute to the pathogenesis of TR in cats.

Declarations

Ethical Approval Not applicable.

Consent to Participate Not applicable.

Consent to Publish Not applicable.

Competing Interests The authors indicate no potential conflicts of interest.

References

1. Lommer, M. J., & Verstraete, F. J. M. (2000). Prevalence of odontoclastic resorption lesions and periapical radiographic lucencies in cats: 265 cases (1995–1998). *Journal of the American Veterinary Medical Association, 217*, 1866–1869.

2. Ingham, K. E., Gorrel, C., Blackburn, J., & Farnsworth, W. (2001). Prevalence of odontoclastic resorptive lesions in a population of clinically healthy cats. *Journal of Small Animal Practice, 42*, 439–443.

3. Collados, J., Garcia, C., Soltero-Rivera, M., & Rice, C. A. (2018). Dental Pathology of the Iberian Lynx (*Lynx pardinus*), Part II: Periodontal Disease, Tooth Resorption, and Oral Neoplasia. *Journal of Veterinary Dentistry, 35*, 209–216.

4. Aghashani, A., Kim, A. S., Kass, P. H., & Verstraete, F. J. M. (2016). Dental Pathology of the California Bobcat (Lynx rufus californicus). *Journal of Comparative Pathology, 154*, 329–340.

5. Aghashani, A., Kim, A. S., Kass, P. H., & Verstraete, F. J. M. (2017). Dental and Temporomandibular Joint Pathology of the California Mountain Lion (Puma concolor couguar). *Journal of Comparative Pathology, 156*, 251–263.

6. Lee, S., et al. (2020). Transcriptomic profiling of feline teeth highlights the role of matrix metalloproteinase 9 (MMP9) in tooth resorption. *Science and Reports, 10*, 18958.

7. Booij-Vrieling, H. E., et al. (2012). Osteoclast progenitors from cats with and without tooth resorption respond differently to 1,25-dihydroxyvitamin D and interleukin-6. *Research in Veterinary Science, 92*, 311–316.

8. Girard, N., Servet, E., Hennet, P., & Biourge, V. (2010). Tooth Resorption and Vitamin D $_3$ Status in Cats Fed Premium Dry Diets. *Journal of Veterinary Dentistry, 27*, 142–147.

9. Gorrel, C. (2015). Tooth resorption in cats: Pathophysiology and treatment options. *Journal of Feline Medicine and Surgery, 17*, 37–43.

10. DeLaurier, A., Boyde, A., Jackson, B., Horton, M. A., & Price, J. S. (2009). Identifying early osteoclastic resorptive lesions in feline teeth: A model for understanding the origin of multiple idiopathic root resorption. *Journal of Periodontal Research, 44*, 248–257.

11. Chu, E. Y., et al. (2021). Multiple Idiopathic Cervical Root Resorption: A Challenge for a Transdisciplinary Medical-Dental Team. *Frontiers in Dental Medicine, 2*, 652605.

12. Wu, J., et al. (2016). Multiple idiopathic cervical root resorption: A case report. *International Endodontic Journal, 49*, 189–202.

13. von Arx, T., Schawalder, P., Ackermann, M., & Bosshardt, D. D. (2009). Human and Feline Invasive Cervical Resorptions: The Missing Link?—Presentation of Four Cases. *Journal of Endodontia, 35*, 904–913.

14. Fawzy-El-Sayed, K., Mekhemar, M., Adam-Klages, S., Kabelitz, D. & Dorfer, C. (2016). TlR expression profile of human gingival margin-derived stem progenitor cells. *Medicina Oral, Patología Oral y Cirugía Bucal* e30–e38. https://doi.org/10.4317/medoral.20593.

15. Sun, Q., Nakata, H., Yamamoto, M., Kasugai, S., & Kuroda, S. (2019). Comparison of gingiva-derived and bone marrow mesenchymal stem cells for osteogenesis. *Journal of Cellular and Molecular Medicine, 23*, 7592–7601.

16. Solis-Castro, O. O., Rivolta, M. N., & Boissonade, F. M. (2022). Neural Crest-Derived Stem Cells (NCSCs) Obtained from Dental-Related Stem Cells (DRSCs): A Literature Review on Current Knowledge and Directions toward Translational Applications. *International Journal of Molecular Sciences, 23*, 2714.

17. Kim, D., Lee, A. E., Xu, Q., Zhang, Q., & Le, A. D. (2021). Gingiva-Derived Mesenchymal Stem Cells: Potential Application in Tissue Engineering and Regenerative Medicine - A Comprehensive Review. *Frontiers in Immunology, 12*, 667221.

18. Sun, Q., Nakata, H., Yamamoto, M., Kasugai, S., & Kuroda, S. (2019). Comparison of gingiva-derived and bone marrow mesenchymal stem cells for osteogenesis. *Journal of Cellular and Molecular Medicine, 23*, 7592–7601.

19. Solis-Castro, O. O., Rivolta, M. N., & Boissonade, F. M. (2022). Neural Crest-Derived Stem Cells (NCSCs) Obtained from Dental-Related Stem Cells (DRSCs): A Literature Review on Current Knowledge and Directions toward Translational Applications. *International Journal of Molecular Sciences, 23*, 2714.

20. Tóthová, L., & Celec, P. (2017). Oxidative Stress and Antioxidants in the Diagnosis and Therapy of Periodontitis. *Frontiers in Physiology, 8*, 1055.

21. Kornicka, K., Szłapka-Kosarzewska, J., Śmieszek, A., & Marycz, K. (2019). 5-Azacytydine and resveratrol reverse senescence and ageing of adipose stem cells via modulation of mitochondrial dynamics and autophagy. *Journal of Cellular and Molecular Medicine, 23*, 237–259.

22. Marycz, K., Weiss, C., Śmieszek, A., & Kornicka, K. (2018). Evaluation of Oxidative Stress and Mitophagy during Adipogenic Differentiation of Adipose-Derived Stem Cells Isolated from Equine Metabolic Syndrome (EMS) Horses. *Stem Cells Intenational, 2018*, 5340756.

23. Weiss, C., Kornicka-Grabowska, K., Mularczyk, M., Siwinska, N., & Marycz, K. (2020). Extracellular Microvesicles (MV's) Isolated from 5-Azacytidine-and-Resveratrol-Treated Cells Improve Viability and Ameliorate Endoplasmic Reticulum Stress in Metabolic Syndrome Derived Mesenchymal Stem Cells. *Stem Cell Reviews and Reports, 16*, 1343–1355.

24. Vono, R., Jover Garcia, E., Spinetti, G. & Madeddu, P. (2018). Oxidative Stress in Mesenchymal Stem Cell Senescence: Regulation by Coding and Noncoding RNAs. *Antioxidants & Redox Signaling.* **9**, 864–879.

25. Marycz, K., Grzesiak, J., Wrzeszcz, K., & Golonka, P. (2012). Adipose stem cell combined with plasma-based implant bone tissue differentiation in vitro and in a horse with a phalanx digitalis distalis fracture: A case report. *Veterinární Medicína, 57*, 610–617.

26. The Modified Triadan System: Nomenclature for Veterinary Dentistry - Michael R. Floyd. (1991). https://journals.sagepub.com/doi/10.1177/089875649100800402.

27. Marycz, K., Toker, N. Y., Grzesiak, J., Wrzeszcz, K. & Golonka, P. (2012). The therapeutic effect of autogenic adipose derived stem cells combined with autogenic platelet rich plasma in tendons disorders hi horses in vitro and in vivo research. *Journal of Animal and Veterinary Advances, 11*(23), 4324-4331. https://doi.org/10.3923/javaa.2012.4324.4331

28. Marycz, K., Kornicka, K., & Röcken, M. (2018). Static Magnetic Field (SMF) as a Regulator of Stem Cell Fate – New Perspectives in Regenerative Medicine Arising from an Underestimated Tool. *Stem Cell Reviews and Reports, 14*, 785–792.

29. Arzi, B., et al. (2020). A multicenter experience using adipose-derived mesenchymal stem cell therapy for cats with chronic, non-responsive gingivostomatitis. *Stem Cell Research & Therapy, 11*, 115.

30. Arzi, B., et al. (2016). Therapeutic Efficacy of Fresh, Autologous Mesenchymal Stem Cells for Severe Refractory Gingivostomatitis in Cats. *Stem Cells Translational Medicine, 5*, 75–86.

31. Arzi, B., et al. (2017). Therapeutic Efficacy of Fresh, Allogeneic Mesenchymal Stem Cells for Severe Refractory Feline Chronic Gingivostomatitis. *Stem Cells Translational Medicine, 6*, 1710–1722.

32. Kim, H.-R., et al. (2017). Extensive characterization of feline intra-abdominal adipose-derived mesenchymal stem cells. *Journal of Veterinary Science, 18*, 299–306.

33. Grzesiak, J., Marycz, K., Wrzeszcz, K., & Czogała, J. (2011). Isolation and Morphological Characterisation of Ovine

Adipose-Derived Mesenchymal Stem Cells in Culture. *International Journal of Stem Cells, 4*, 99–104.

34. Jin, S. H., et al. (2015). Isolation and characterization of human mesenchymal stem cells from gingival connective tissue. *Journal of Periodontal Research, 50*, 461–467.

35. Grzesiak, J., Marycz, K., Czogala, J., Wrzeszcz, K., & Nicpon, J. (2011). Comparison of Behavior, Morphology and Morphometry of Equine and Canine Adipose Derived Mesenchymal Stem Cells in Culture. *International Journal of Morphology, 29*, 1012–1017.

36. Peters, E. B., Christoforou, N., Moore, E., West, J. L., & Truskey, G. A. (2015). CD45+ Cells Present Within Mesenchymal Stem Cell Populations Affect Network Formation of Blood-Derived Endothelial Outgrowth Cells. *BioResearch Open Access, 4*, 75–88.

37. Liu, J., et al. (2019). Periodontal Bone-Ligament-Cementum Regeneration via Scaffolds and Stem Cells. *Cells, 8*, 537.

38. Chen, Y., & Liu, H. (2016). The differentiation potential of gingival mesenchymal stem cells induced by apical tooth germ cell-conditioned medium. *Molecular Medicine Reports, 14*, 3565–3572.

39. Cho, Y.-D., Kim, K.-H., Lee, Y.-M., Ku, Y., & Seol, Y.-J. (2021). Periodontal Wound Healing and Tissue Regeneration: A Narrative Review. *Pharmaceuticals, 14*, 456.

40. Ouchi, T., & Nakagawa, T. (2020). Mesenchymal stem cell-based tissue regeneration therapies for periodontitis. *Regenerative Therapy, 14*, 72–78.

41. Oestreich, A. K., Collins, K. H., Harasymowicz, N. S., Wu, C.-L., & Guilak, F. (2020). Is Obesity a Disease of Stem Cells? *Cell Stem Cell, 27*, 15–18.

42. Tomasello, L., et al. (2017). Mesenchymal stem cells derived from inflamed dental pulpal and gingival tissue: A potential application for bone formation. *Stem Cell Research & Therapy, 8*, 179.

43. Tang, L., Li, N., Xie, H., & Jin, Y. (2011). Characterization of mesenchymal stem cells from human normal and hyperplastic gingiva. *Journal of Cellular Physiology, 226*, 832–842.

44. Antonioli, L., Pacher, P., Vizi, E. S., & Haskó, G. (2013). CD39 and CD73 in immunity and inflammation. *Trends in Molecular Medicine, 19*, 355–367.

45. Otabe, K., et al. (2012). Comparison of Gingiva, Dental Pulp, and Periodontal Ligament Cells From the Standpoint of Mesenchymal Stem Cell Properties. *Cell Medicine, 4*, 13–21.

46. Frontiers | Multiple Idiopathic Cervical Root Resorption: A Challenge for a Transdisciplinary Medical-Dental Team. https://www.frontiersin.org/articles/10.3389/fdmed.2021.652605/full.

47. Page, R. C., & Baab, D. A. (1985). A new look at the etiology and pathogenesis of early-onset periodontitis. Cementopathia revisited. *Journal of Periodontology, 56*, 748–751.

48. Arnett, T. R., et al. (2003). Hypoxia is a major stimulator of osteoclast formation and bone resorption. *Journal of Cellular Physiology, 196*, 2–8.

49. Al-Rawi, N. H., Al-Marzooq, F., Al-Nuaimi, A. S., Hachim, M. Y., & Hamoudi, R. (2020). Salivary microRNA 155, 146a/b and 203: A pilot study for potentially non-invasive diagnostic biomarkers of periodontitis and diabetes mellitus. *PLoS ONE, 15*, e0237004.

50. Ma, F. et al. (2022). The role of Nrf2 in periodontal disease by regulating lipid peroxidation, inflammation and apoptosis. *Frontiers in Endocrinology*, *13*. https://doi.org/10.3389/fendo.2022.963451

51. Liu, J., Wang, X., Xue, F., Zheng, M., & Luan, Q. (2022). Abnormal mitochondrial structure and function are retained in gingival tissues and human gingival fibroblasts from patients with chronic periodontitis. *Journal of Periodontal Research, 57*, 94–103.

52. Pang, Y., Zhang, C., & Gao, J. (2021). Macrophages as Emerging Key Players in Mitochondrial Transfers. *Frontiers in Cell and Development Biology, 9*, 747377.